Experiments in Fluids 26 (1999) 441–450 © Springer-Verlag 1999

Conditional sampling and state space reconstruction

A. Porporato

Abstract This work looks into the existing links between conditional sampling techniques for coherent structure identification and methods for state space reconstruction which come up in the field of nonlinear time series analysis. It is shown that the sampling condition used by the VITA method corresponds to a round hyper-cylinder, having as its axis the main diagonal of an embedding space reconstructed with the delay method. Such a geometrical interpretation allows us to better understand certain typical characteristics of the method and to see bursting events as excursions of the system leaving the high-dimension basic turbulence.

1
Introduction

The identification of coherent structures (for an outline see Robinson 1991) in a turbulent flow field is a far from simple operation, as the coherent and non-coherent components in a turbulent field co-exist and dynamically interact (Hussain 1986). Therefore, in order to identify the coherent structures and give them a suitable description it is fundamental to have the most detailed knowledge possible of the flow field. In many cases, however, only a scalar time series measured at a single point in the flow is available. With such a limitation the difficulty of coherent structure identification considerably increases and the objective must be reduced to looking for characteristic signs of coherent structures in the available series. To this purpose a large number of methods using the most diversified instruments of time series analysis have been proposed (e.g. Bonnet 1995).

Among these methods, the present paper will deal with those known as conditional sampling (Antonia 1981), investigating the links between these and the techniques for state space reconstruction, which are the basis of modern nonlinear time series analysis (e.g. Grassberger et al. 1991; Abarbanel et al. 1993). These latter techniques, at least from a theoretical point of view, allow us to reconstruct the dynamics of a system in a space topologically equivalent to the actual phase space, starting with only a single time series. In such a space, known as embedding space, the information contained in the series becomes more accessible, and consequently the detection of the coherent structure also proves to be more profitable. Thanks to the link between state space reconstruction and conditional sampling, it is possible to re-interpret some of the most recognised methods of conditional sampling. Further on, we will focus especially on the VITA method (Blackwelder and Kaplan 1976), to show how the operations carried out on the data correspond to a state space reconstruction and how in the embedding space its sampling condition has interesting geometrical and physical interpretations.

2
State space reconstruction

The state space reconstruction of a system from the knowledge of a single scalar variable is one of the fundamental problems of the nonlinear time series analysis (e.g. Grassberger et al. 1991; Abarbanel et al. 1993). It is based on the general consideration that the interaction between the variables is such that each component contains information on the complex dynamics of the system and that consequently, even by measuring only one of the variables that govern the system, it is possible to reconstruct a space which is topologically equivalent to the real phase space (Packard et al. 1980; Takens 1981; Sauer et al. 1991).

Although in practice the reconstruction can be obstructed by the presence of noise and by the brevity of the series available (Casdagli et al. 1991), the reconstruction techniques have been successfully applied to the time series of low-dimension chaotic systems. One cannot say the same thing of systems (such as fully turbulent flows) characterised by a high level of spatio-temporal complexity. For such systems, the methods of nonlinear time series analysis are still only in their preliminary stages (Abarbanel et al. 1993; Cross and Hohenberg 1993) and their dynamics has a dimension which is too high to be comprehensively reconstructed applying the available methods to a single scalar series. However, even if one must be cautious of the limitations of nonlinear analysis for turbulent time series, one should not be too discouraged. In fact, also in this case with the correct application of the reconstruction techniques we can obtain an embedding space which, although not equivalent to the real phase space of the system, allows us to well take advantage of the information present in the time series. In such space the analysis of the time series is more

Received: *10 October 1997*/*Accepted*: *4 November 1998*

A. Porporato
Dipartimento di Idraulica Trasporti e Infrastrutture Civili
Politecnico di Torino, Corso Duca degli Abruzzi, 24
I-10129 Torino, Italy

Correspondence to: A Porporato

I wish to thank Luca Ridolfi for invaluable help and advice. The assistance given by referees is also gratefully acknowledged.

profitable and consequently, as already observed in part by Keefe (1988), the identification of coherent structures also proves to be more effective.

2.1
The delay method

The delay time method of Takens (1981; see also Packard et al. 1980; Sauer et al. 1991) is the most common method for state space reconstruction (e.g. Grassberger et al. 1991; Abarbanel et al. 1993). Choosing a suitable delay time τ (usually a multiple of the sampling interval Δt, i.e. $\tau = J\Delta t$), the method entails the construction from the shear time series $u_i = u(t_i) = u(t_0 + i\Delta t)$, $i = 0, \ldots, N-1$, of a set of $M = N - (m-1)\tau/\Delta t$ m-dimensional vectors of the form

$$\mathbf{u}_i = \{u_i, u_{i-J}, u_{i-2J}, \ldots, u_{i-(m-1)J}\} \quad (1)$$

where m is the embedding dimension. Equation (1) is the original form but, in general, the Takens method can utilise information both on the present and on the future, according to the so-called mixed reconstruction (Casdagli et al. 1991)

$$\mathbf{u}_i = \{u_{i-\alpha_p J}, \ldots, u_{i-J}, u_i, u_{i+J}, \ldots, u_{i+\alpha_f J}\} \quad (2)$$

with $m = \alpha_p + 1 + \alpha_f$. When $\alpha_f = 0$ Eq (1) is re-obtained and the reconstruction is said to be predictive. If $m \geqslant 2D+1$ (where D is the fractal dimension of the attractor) such vectors describe an object topologically equivalent to the attractor of the physical system from which u has been measured. Apart from these conditions concerning the value of m there should not be any other limits to the choice of the parameters m and τ. In practice, however, as Takens theory pre-supposes a noiseless series of infinite length, the application of the method proves to be heuristic. The quality of the reconstruction depends on τ and m and their combination, $\tau_w = (m-1)\tau$, which is the width of the reconstruction window. The values of the optimal embedding parameters depend on the compromise of contrasting requirements: firstly, m must exceed by at least twice the dimensions of the attractor (for some types of analysis Sauer et al. (1991) have shown that it is sufficient that m is greater than D); furthermore τ must be sufficiently great to not involve data which is too correlated in such a way that the supply of new information is superior to the noise level in the series. Finally, τ must not be so great as to sample data too distant in time and therefore (if the system is chaotic) with a dynamic link which by then is too weak (see Casdagli et al. 1991). Thus, the choice of optimal embedding parameters is by no means simple and, even if numerous methods have been proposed (see Rosenstein et al. (1994) for a review), there does not seem to be one which is in any way preferable.

As shown by Casdagli et al. (1991), the quality of the reconstruction proves to be lower the higher the complexity of the system and the noise level in the series are. As a result the dynamic reconstruction is only totally feasible for chaotic systems of low dimensions, while for systems of a higher dimension (as fully turbulent flows certainly are) it can only be partially feasible, in that it is not possible to reach sufficient values of m to totally unfold the attractor. For this reason, therefore, it is advisable to firstly determine τ_w and, only following that, within the established reconstruction window, choose the values of m and τ. It is clear that in this second phase, high values of m are generally preferable, even if (with τ_w constant) the contemporary reduction of τ makes the addition of new variables less and less significant and can even cause disturbances which reduce the quality of the reconstruction. This was evident in the paper by Porporato and Ridolfi (1997), where it was observed that beyond a certain value of m the quality of the prediction (strictly linked to the quality of the reconstruction) carried out with τ constant ceased to improve because of the extension of the window width. Furthermore, too large values of m can excessively aggravate the calculation burden to the point that any benefits obtainable would be considered unjustifiable.

In this work, we will only take into account the method of Takens. Other methods of state space reconstruction do exist (see Abarbanel et al. 1993), among which we recall that of the successive derivatives and that based on the principal component analysis. Gibson et al. (1992) demonstrated the close link that exists between these different methods.

2.2
Application to measured turbulent series

The variable under examination is the near-wall longitudinal velocity component, indicated as usual as $u(t)$, measured using a Laser Doppler Anemometer in smooth-pipe flows with Reynolds numbers (calculated using the mean bulk velocity and the diameter of the pipe) equal to 7000 and 15000. The measurement point is placed in the buffer region, where the maximum production of turbulence is found, at $y^+ = yu_*/\nu = 15$, where y is the distance from the wall, u_* the friction velocity and ν the kinematic viscosity (hereafter, the variables with '+' indicate the adimensionalization with the 'wall' variables u_* and ν). For details about the description of the experimental apparatus or on the preliminary elaborations, one can refer to Porporato and Ridolfi (1997).

To standardise the sampling features of the two series and to make the comparison between the elaborations more coherent, the following analyses are based on tracts lasting approximately 10000 temporal 'wall' units ($t^+ = tu_*^2/\nu$), that assure a sufficient number of bursting events in the series. The number of points, the duration of the series and the time interval between the data (these two latter in temporal 'wall' units) respectively proved to be equal to 30883, 9905 and 0.321 for the series with $Re = 7000$ and equal to 23750, 10780 and 0.451 for that with $Re = 15000$. In dimensional terms, this corresponds to a measure of duration of 999 s for $Re = 7000$ and of 290 s for $Re = 15000$. Figure 1 shows the initial part of the two velocity series. The irregular and intermittent behaviour with prevalently strong positive gradients is typical of near-wall turbulent series.

In order to determine the optimal embedding parameters, two methods for the assessment of τ have been applied. The first of these is the fill factor method (Buzug and Pfister 1992). According to it, the optimum τ is chosen corresponding to the first maximum of the fill-factor function, defined as the logarithm of the average volume of all m-dimensional parallelepipeds, given by the points of the attractor. The second method adopted is based on the consideration that a correct reconstruction should ensure the maximum possible separation between trajectories (Buzug and Pfister 1992). Details of the application of these methods are given in Porporato and Ridolfi (1997). The results, which provide an upper bound to

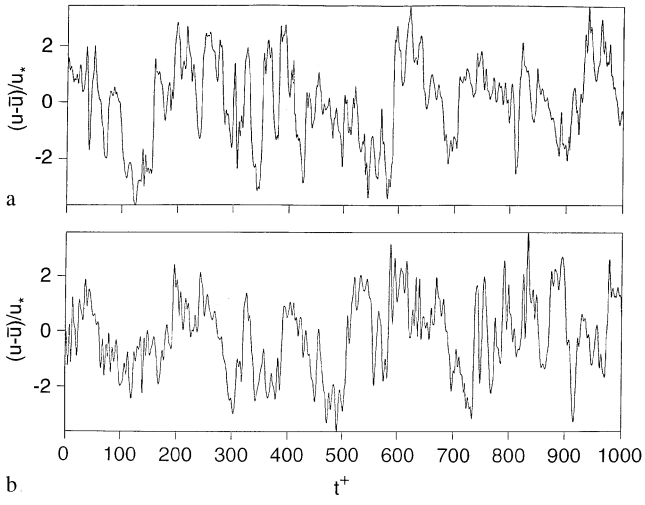

Fig. 1a,b. Traces of the initial part of the turbulent velocity time series, normalized with the 'wall' variables. **a** $Re=7000$; **b** $Re=15000$

Table 1. Optimal delay-times

	$Re=7000$	$Re=15000$
Fill factor (τ^+)	$\leqslant 1.9-2.2$	$\leqslant 2.2-2.7$
Maximum spreading (τ^+)	$\leqslant 1.6-2.2$	$\leqslant 1.8-2.7$
Average displacement (τ_w^+)	≈ 7 ($m>10-12$)	≈ 8 ($m>10-12$)
Critical window width (τ_w^+)	≈ 8	≈ 8

the choice of the optimum values of τ, are for both methods of around $\tau^+=2$ and 2.5 respectively for $Re=7000$ and $Re=15000$ (Table 1).

Since in high dimension systems the value of τ_w is more important than the value of τ, the methods of the critical window width (Gibson et al. 1992) and of average displacement (Rosenstein et al. 1994) were also applied. These were specifically proposed to estimate the critical window width of the reconstruction. According to the first of these, the value of τ_w is chosen as a fraction of the critical window width, τ_w^*, which represents the window width below which the eigenvectors of the principal component analysis correspond (to the leading order) to Legendre polynomials, i.e.

$$\tau_w=\mu\tau_w^*=2\mu\sqrt{\frac{3\overline{u^2}}{(\mathrm{d}u/\mathrm{d}t)^2}} \tag{3}$$

where the over bar denotes a time average over the entire length of the series. (We presume to use series from which the mean value has already been subtracted; in such a case $\overline{u^2}$ represents the signal variance, whose square root, u', is the standard deviation.) Based on empirical results, Gibson et al. (1992) suggest that $\mu=0.5$ provides good results. The advantages of this method are the facility and speed in implementation and its solid theoretical foundations, while on the other hand, the need to numerically estimate the derivative of the signal can run the risk of noise amplification. In this application, working on signals which are already noise reduced, the trials carried out using different formulae of numerical derivation have provided practically coincident results. It is interesting to note that the critical window width proves to be both proportional and close to the Taylor time microscale (Tennekes and Lumley 1972, pg. 211), being

$$\tau_w^*=\sqrt{6}\lambda \tag{4}$$

Since λ represents the intercept of the parabola that matches the autocorrelation at the origin, the recommended value of τ_w can also be expressed using the autocorrelation of the signal.

The method of average displacement (Rosenstein et al. 1994) is a method of geometrical type that provides a value of τ_w ensuring an average expansion of the reconstruction sufficient to well unfold the attractor. The values are chosen when for a given m, the slope of the curve of the distance from the identity line or main diagonal at the growth of τ reaches 40% of its original value. It is necessary to underline, particularly in view of what will be said in the following, that the average displacement proposed by Rosenstein et al.,

$$\overline{S_m(\tau)}=\frac{1}{M}\sum_{i=1}^{M}\sqrt{\sum_{j=1}^{m-1}(u_{i-J_j}-u_i)^2} \tag{5}$$

is not precisely the distance from the main diagonal (which will be introduced in Sect. 3), but the distance from it taken on the hyper-plane $u_i=const.$

The results of the application of these last two methods are in agreement between themselves (Table 1), with values of τ_w^+ around 7–8. Since for high dimension systems the constraints on τ_w are stronger than for that on τ, it is most probable that the best reconstructions are those where, without exceeding the τ_w obtained, values of τ^+ below 2 (contrary to what would be required for fill factor and maximum spreading of trajectories methods) are used, thus applying values of m which are greater than 4. In other words, it is preferable to use a greater number of co-ordinates with delay time lower than the optimal (and so with a lesser supply of information for single co-ordinates) rather than a too low, even if dynamically more significant, number of co-ordinates.

An indication of the quality of the reconstructions can be taken from the analysis of the two-dimensional representations obtained from the two time series (Figs. 2a and b). The projections are similar and reveal evidence of arch-shaped trajectories in the upper part. Theses are due to the intense positive gradients present in the series and, as we will see, are linked to the bursting events detected by the VITA technique.

3
The VITA method

Following the definition of Antonia (1981), 'conditional sampling' is a mean to distinguish and provide quantitative information about interesting regions of a turbulent flow. As suggested by the name itself, it associates the presence of a coherent structure with the verification of particular 'conditions' in the time series. Some these methods usually involve subsequent values of the time series, it is logial to think that the conditions imposed on the time series have a geometrical equivalent in the embedding space. We will attempt to look more deeply into this link for one of the most efficient and practised methods of conditional sampling: the VITA method.

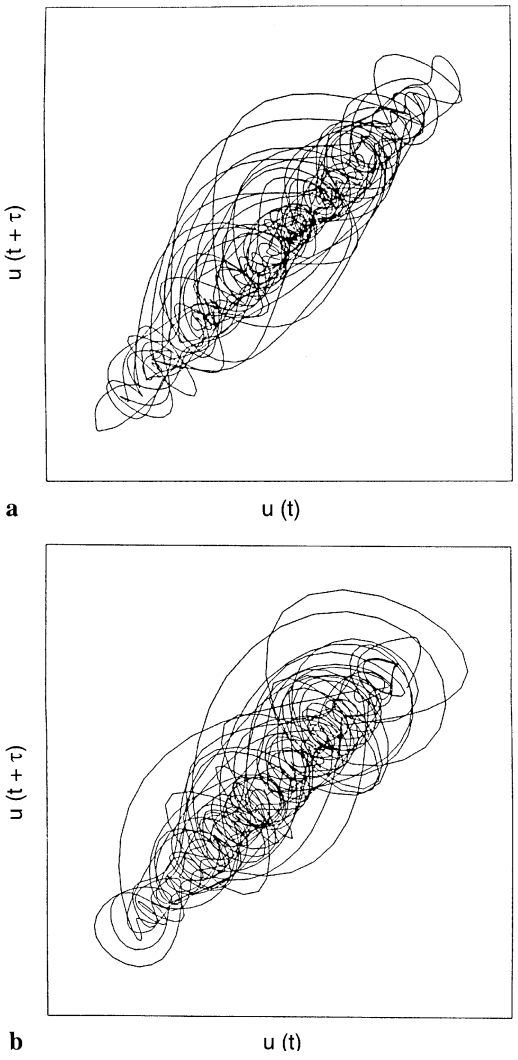

Fig. 2a,b. Two-dimensional reconstructions in the plane $\{u(t), u(t+\tau)\}$. **a** $Re=7000$, $\tau^+=2$; **b** $Re=15000$, $\tau^+=2$

The VITA method (Blackwelder and Kaplan 1976) focuses on tracts of strong fluctuation of the longitudinal velocity component. The Variable Interval Time Average of the quantity $u(t)$ is defined as

$$\overline{u(t)}_T=\frac{1}{T}\int_{t-T/2}^{t+T/2} u(s)\,\mathrm{d}s \tag{6}$$

In a similar way, the local variance is

$$\overline{\mathrm{var}(t)}_T=\overline{(u-\bar{u}_T)^2}_T=\overline{u_T^2}-\bar{u}_T^2 \tag{7}$$

When the value of $\overline{\mathrm{var}(t)}_T$ is high, the signal shows intense and rapid fluctuations that for brief integration intervals correspond to intense gradients. In the frequency domain, the link between the signal and local variance is not immediate: numerical tests carried out on a white noise show that it actually should correspond to a low-pass filter (similar to that of the moving average) with a slope and modulation proportional to $1/T$.

$\overline{\mathrm{var}(t)}_T$ is the new turbulent variable on which the conditional sampling is carried out, defining a detection function

$$D(t)=\begin{cases}1 & \text{if } \overline{\mathrm{var}(t)}_T \geqslant K\overline{u^2}\\ 0 & \text{otherwise}\end{cases} \tag{8}$$

where T and K are the parameters of the method. Since the method is quite sensitive to the threshold values and there are no objective criteria concerning their specification, an adjustment is generally made by comparison with visualizations. We will return later on to VITA parameters.

The success of the VITA method is essentially due to the ease of implementation and to the good correspondence between its detections and the second quadrant events that correspond to peaks in turbulent production (ejections). These latter are, in fact, generally included between intense gradients (Alfredsson and Johansson 1984) detected by the VITA which can be interpreted as internal shear layers (Landahl 1990). Recently Jeong et al. (1997) drew attention to the link between the typical behaviour of VITA detections and the near-wall passage of highly elongated quasi-streamwise vortices, while Tardu (1995) observed the existence of two different types of VITA events divided in single and multiple shear layers and characterised by a different regeneration mechanism.

3.1
The VITA method in the embedding space

We now show that the VITA method has an interesting correspondence in the embedding space. To this purpose, let us introduce a mixed reconstruction, centered on the i-th point and realised with $\tau=1$,

$$\mathbf{u}_i=\{u_{i-\alpha},\ \ldots,\ u_{i-1},\ u_i,\ u_{i+1},\ \ldots,\ u_{i+\alpha}\} \tag{9}$$

where $\alpha=(m-1)/2$, and write the discrete version of the local variance centring the sum on u_i

$$\overline{\mathrm{var}(t)}_{i,m}=\frac{1}{m}\sum_{j=-\alpha}^{\alpha}u_{i+j}^2-\left(\frac{1}{m}\sum_{j=-\alpha}^{\alpha}u_{i+j}^2\right)^2 \tag{10}$$

having set $T=m\,\Delta t$. (Notice that the choice of an uneven m and the use of a mixed reconstruction are solely finalised to make the notation coherent and do not represent a limitation.) It now is easy to show that in the embedding space of dimension m, $\overline{\mathrm{var}(t)}_{i,m}$ is a simple function of the distance of the point $\mathbf{u}_i$ from the main diagonal. The distance d_i between the point $\mathbf{u}_i$ and the generic point $\mathbf{u}_b$ of the main diagonal is written as

$$d_i(u_b)=\|\,\mathbf{u}_i-\mathbf{u}_b\,\|_2=\sqrt{\sum_{j=-\alpha}^{\alpha}(u_{i+j}-u_b)^2} \tag{11}$$

Minimising the distance with respect to u_b, we obtain

$$u_{b,\min}=\frac{1}{m}\sum_{j=-\alpha}^{\alpha}u_{i+j} \tag{12}$$

which substituted in (11) gives the distance of $\mathbf{u}_i$ from the main diagonal

$$d_i(u_b)=\sqrt{\sum_{j=-\alpha}^{\alpha}\left(u_{i+j}-\frac{1}{m}\sum_{j=-\alpha}^{\alpha}u_{i+j}\right)^2} \tag{13}$$

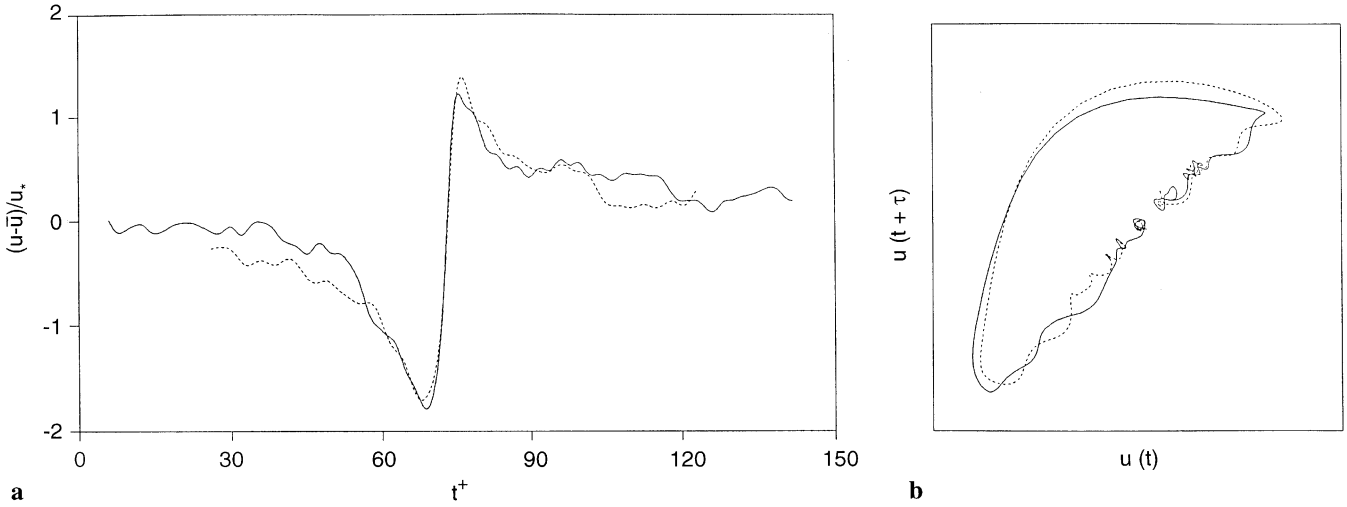

Fig. 3. a Traces of the averaged velocity profiles during VITA detections; **b** relative two-dimensional reconstructions in the plane $\{u(t), u(t+\tau)\}$, using the same delay times as in Fig. 2a–b. Solid lines refer to $Re=7000$, broken lines to $Re=15000$

Finally, we can make the expression of the local variance appear in (13) to have

$$d_i(u_b)=\sqrt{m}\sqrt{\frac{1}{m}\sum_{j=-\alpha}^{\alpha}u_{i+j}^2-\left(\frac{1}{m}\sum_{j=-\alpha}^{\alpha}u_{i+j}\right)^2}=\sqrt{m}\sqrt{\mathrm{var}_{i,m}} \tag{14}$$

The VITA method therefore associates the presence of coherent structures to the distancing of the representative point from the main diagonal. The condition (8), in the embedding space reconstructed according to (9), thus corresponds to a round hyper-cylinder having the main diagonal as its axis and a radius of $\sqrt{mK}u'$. This becomes evident in embedding spaces of smaller dimensions. Letting, to be brief $u_{i-1}=x$, $u_i=y$, $u_{i+i}=z$, when $m=2$ one has $\overline{\mathrm{var}_2}=(x-y)^2/4 \geqslant K\overline{u^2}$, which determines the points distant at least $\sqrt{2K}u'$ from the main diagonal, while for $m=3$ one has

$$\overline{\mathrm{var}_3}=(x^2+y^2+z^2-xy-xz-yz)/9\geqslant K\overline{u^2} \tag{15}$$

which corresponds to sampling external points with respect the round cylinder having the main diagonal as its axis and radius $\sqrt{3K}u'$.

The geometrical interpretation in the embedding space enables us to give an interesting physical interpretation of the conditional sampling achieved by VITA, that would correspond to the idea of coherent structure as an orbit which distances itself from the high-dimensional central body of the attractor, similarly to what happens in the bursting model hypothesised by Newell et al. (1988) and in the low dimension model of Aubry et al. (1988). (Although there is no demonstration that wall turbulence has an attractor, here such a term is used loosely to indicate the object that the system describes in its phase space.) Figure 3 shows the conditionally-averaged velocity obtained by aligning the VITA detections at the maximum gradient and the relative two-dimensional projections of the plane $\{u(t), u(t+\tau)\}$. The arch-shaped behaviour already found in the projections of the series (Figs. 2a and b) is even more evident and shows the typical excursion during bursting events when the system leaves the central body of the attractor relative to the basic turbulence.

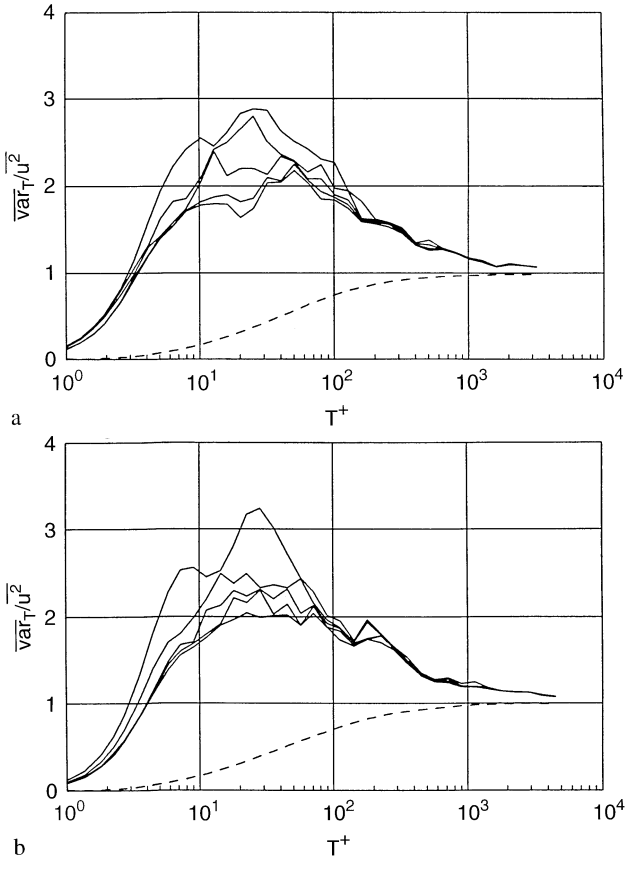

Fig. 4a,b. Values of the first five maxima (solid lines) and of the mean (broken line) of the local variance versus the window width T. **a** $Re=7000$; **b** $Re=15000$

3.2
VITA thresholds and embedding parameters

As we have seen, the VITA parameter T corresponds to the windows width τ_w of the reconstruction and, being $\tau = 1$, also to the embedding dimension m. Therefore, by varying T and maintaining K constant, we can study the influence of m on the reconstruction of the attractor and, as a result, on the VITA detections. Since T governs the way in which the attractor expands with respect to the VITA cylinder, by improving the reconstruction with a correct choice of the embedding parameters, the reliability of the method should also improve.

The criteria of average displacement and critical window width gave for both series $\tau_w^+ \approx 7-8$, which is slightly underestimated with respect to the values usually recommended in literature for T^+ (see Luchik and Tiedermann 1987 and Yuan et al. 1994). The reason for this may be related to the fact that, differently from VITA, the employed criteria for choosing τ_w are not based directly on the real distance from the main diagonal of the embedding space, whilst the most appropriate variable for the choice of T is the distance from the main diagonal or, equivalently, the local variance $\overline{\mathrm{var}(t)_T}$. To this regard, Figs. 4a and b show the behaviour of the first five maxima and the mean of $\overline{\mathrm{var}(t)_T}$ versus the window width. While the mean value proves to be always increasing, without indicating whether the expansion corresponds to an effective better unfolding of the attractor, the maxima present a peak indicating the existence of particular reconstructions giving maximum expansion of the most external orbits and, therefore, also maximum efficiency of the conditional sampling. Figure 5 reports the difference between the curves of the mean values of the first five maxima (solid lines in Figs. 4a and b) and that of the mean value of $\overline{\mathrm{var}(t)_T}$ (broken lines in Figs. 4a and b). Either from Figs. 4a and b or from Fig. 5 it can be observed that the reconstruction windows giving maximum separation between external orbits and the main body of the attractor are obtained for T^+ around 10–20. There is then a range of T^+ that assures the best conditional sampling and corresponds quite well to the values recommended in literature. This can represent a possible way for determining the parameter T without having to resort to the comparison with visualizations, making it easier to apply VITA to different kinds of flow and turbulence variables. More generally, the use of $\overline{\mathrm{var}(t)_T}$ in nonlinear time series analysis could be preferable to other methods for the choice of τ_w, such as the average displacement, at least for cases where the system presents different coexisting dynamics.

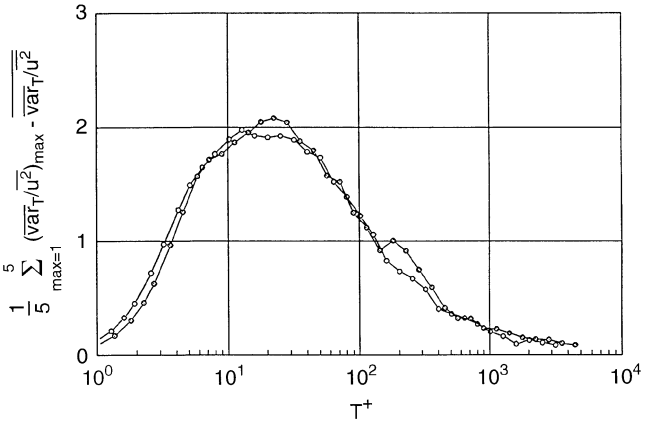

Fig. 5. Difference between the mean of the first five maxima of the local variance and its mean value. $Re = 7000$: open symbols; $Re = 15000$: solid symbols

The behaviour of the number of detections versus T (keeping constant the value of K) is similar to that reported by Johansson and Alfredsson (1982, Figs. 8 and 9). For both series, the number of detections grows up until $T^+ = 20-30$ to then decrease to the point of a single great detection when T is equal to the duration of the entire series. Such a behaviour is easily interpreted in the embedding space where, at first, the increase of T is reflected in the rapid expansion of the attractor whose trajectories progressively come out of the VITA cylinder. Subsequently, the growth rate of the attractor becomes about equal to that of the VITA cylinder (whose radius grows as $\sqrt{m}$). Finally, when T is very high and the local variance tends to the global one, with $K < 1$ the inequality $\overline{\mathrm{var}(t)_T} > K\overline{u^2}$ is always satisfied.

For what concerns the parameter K, we have seen that choosing it corresponds to fixing the radius of the hyper-cylinder defined by VITA. Once T is established, the value of K should separate the part where is more probable to find non-coherent turbulence (inside the cylinder) from that dominated mainly by intense fluctuations of energy relative to the passage of coherent structures (on the outside). Following the attractor scheme proposed by Newell et al. (1988), the radius of the hyper-cylinder should be such to exclude only those orbits that constitute the high dimensional body of the attractor typical of non-coherent turbulence, sampling instead those that correspond to the passage of coherent structures. In effect, even if such a distinction is not clear-cut due to the strong dynamic interconnection between basic turbulence and coherent structures (e.g. Hussain 1986), the p.d.f. of the series of distance from the main diagonal (Figs. 6a and b) shows a double behaviour corresponding to different dynamics in the system. Both graphs present a possible double exponential behaviour indicative of a double family of events: one being much more frequent relative to the trajectories which remain near the main diagonal, the other one being rarer relative to the more distant trajectories. Such two behaviours are underlined by the two straight lines (obtained by the least squares method) relative to the points with a distance lesser or greater than $0.6\,\overline{u^2}$ respectively (the commonly adopted value of K being around 0.6). Even though there is some scatter, probably due to the relatively small number of events detected, there is a region between 0.6 and 1.2 where the passage between the two behaviours takes place. Besides the interest of its physical interpretation, this fact could help in allowing for a choice of the parameter K directly based on the p.d.f. of $\overline{\mathrm{var}(t)_T}$.

We close the discussion on links between VITA and embedding parameters with a brief comment on the role of the embedding dimension m. As previously said, once τ_w is fixed, beyond a certain value of the embedding dimension the quality of the reconstruction does not have substantial improvement by the addition of new variables. This is confirmed in the tests (not shown here) carried out fixing the window width of the reconstruction and applying VITA with values of τ higher than 1. Beyond values of m sufficient to guarantee a good

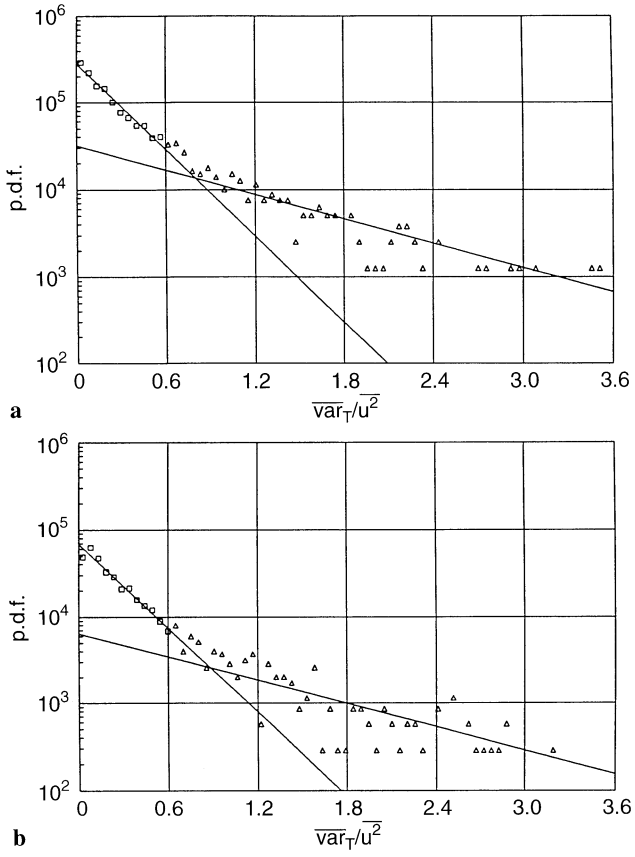

Fig. 6a,b. Probability density functions of the local variance. The straight lines are the regression curves (least squares method) of the points with distance respectively smaller than (open squares) and bigger than (open triangles) $0.6u'$. **a** $Re=7000$; **b** $Re=15000$

reconstruction (about 8–10), the detections practically coincide with those obtained with $\tau=1$. From an applicative point of view, the employment of m which is not too great, can be useful to reduce the calculation times in the case of highly over-sampled signals.

3.3
Higher-order local moments

The geometrical interpretation of the local variance suggests possible extensions in the analysis of turbulent series employing higher-order local moments. The local first-order moment is simply the moving average on tracts of duration T. Imposing a threshold condition on the moving average, one obtains a criterion which is most similar to the ULEVEL method (Lu and Willmarth 1973), with the advantage of a lesser number of false detections because of the filtering of high frequency fluctuations of the signal.

The local third-order central moment (with respect to the local mean)

$$\overline{\mathrm{ter}(t)}_T=\overline{(u-\bar{u}_T)^3}_T=\overline{u^3}_T-3\overline{u^2}_T\bar{u}_T-2\bar{u}_T^2 \tag{16}$$

indicates the degree of asymmetry of the sequence, while that of the fourth order,

$$\overline{\mathrm{quater}(t)}_T=\overline{(u-\bar{u}_T)^4}_T=\overline{u^4}_T-4\overline{u^3}_T\bar{u}_T+6\overline{u^2}_T\bar{u}_T^2-3\bar{u}_T^4 \tag{17}$$

quantifies the degree of intermittency. Before discussing the possible applications, it could be interesting to analyse the geometrical correspondence of (16) and (17) in embedding spaces of lower dimension. In dimension 2, pairs of values having the same mean are found on the line that perpendicularly intersects the main diagonal at the point with co-ordinates equal to the mean. The local variance is given by the square of the distance from the mean diagonal and the entire embedding plane is spanned by two families of perpendicular lines, one relative to the mean of the values and the other to their variance. As information about the time order in the sequence is missing, neither these two quantities are sufficient to clearly identify the pair (two pairs exist with the same mean and variance but with opposite values of the derivative, that are found symmetrically from both parts of the bisector) nor does the definition of higher-order moments add further information, being $\overline{\mathrm{ter}}_2\equiv 0$ and

$$\overline{\mathrm{quater}}_2=\frac{(x-y)^4}{16} \tag{18}$$

which, as the local variance, establishes pairs of parallel lines to the main diagonal. For $m=3$ those sequences having the same mean value and the same local variance rest on the circumference given by the intersection between a perpendicular plane to the main diagonal and a round cylinder which has the same main diagonal as its axis. With the introduction of the asymmetry of the sequence,

$$\overline{\mathrm{ter}}_3=(2x^3-3x^2y-3xy^2+2y^3-3x^2z+12xyz-3y^2-3xz^2-3yz^2+2z^3)/27 \tag{19}$$

a cylinder is established, having the main diagonal as its axis and generatrix of equation

$$\frac{w(-3v^2+w^2)}{3\sqrt{6}}=\mathrm{const} \tag{20}$$

in an orthogonal frame of reference $\{v, w\}$ where the origin of the axes is placed on the trace of the main diagonal and the axis w intersects the old axis z (Fig. 7). On the circumference defined by the mean and the variance, the third-order moment establishes 6 points which constitute the possible combinations

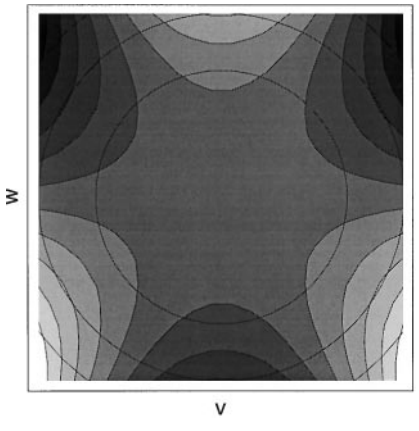

Fig. 7. Contour plot of Eq. (20) showing the generatrixes of the cylinder defined by on a plane orthogonal to the identity line; the VITA-defined circumferences are also shown; see Eq. (15)

of the only three values that give the assigned mean, variance and third-order moment. The fourth-order moment

$$\overline{\text{quater}}_3 = \frac{2(x - xy + y - xz + z)^2}{27} \tag{21}$$

does not add ulterior information, since apart from one constant corresponds to the same family of cylinders defined by the local variance. The fact of dealing with central moments (with respect to the local mean), means that the surfaces defined by them are always cylinders with the main diagonal as their axis. Thanks to this fact, by projecting the equations in a positive orthogonal reference $\{\eta, \zeta, \vartheta, \xi\}$ having the main diagonal as its first axis, it is still possible to have an idea of their form even for $m = 4$. In the new reference such first axis disappears and one obtains

$$\overline{\text{var}}_4 = \frac{\zeta^2 + \vartheta^2 + \xi^2}{4} \tag{22}$$

$$\overline{\text{ter}}_4 = \frac{3(\zeta^2 - \vartheta^2)\,\xi}{8} \tag{23}$$

$$\overline{\text{quarter}}_4 = \frac{2\zeta^4 + 2\vartheta^4 + 6\zeta^2\xi^2 + 6\vartheta^2\xi^2 + \xi^4}{16} \tag{24}$$

As expected, the generatrixes of the local variance are spheres with their centre on the main diagonal, while for the third- and fourth-order moments it is necessary to refer to further sections. Figure 8a shows the family of curves that are obtained by annulling in Eq. (23) ζ or ϑ, while Figs. 8b–d show those which are obtained by annulling in Eq. (24) ζ, ϑ and ξ, respectively. Calculating the local fifth-order moment one can see that this does not give further information, since its relative generatrixes prove to be proportional to the product $\overline{\text{var}}_4 \cdot \overline{\text{ter}}_4$.

The application to turbulent series requires much higher values of m to those which have just been discussed, in order

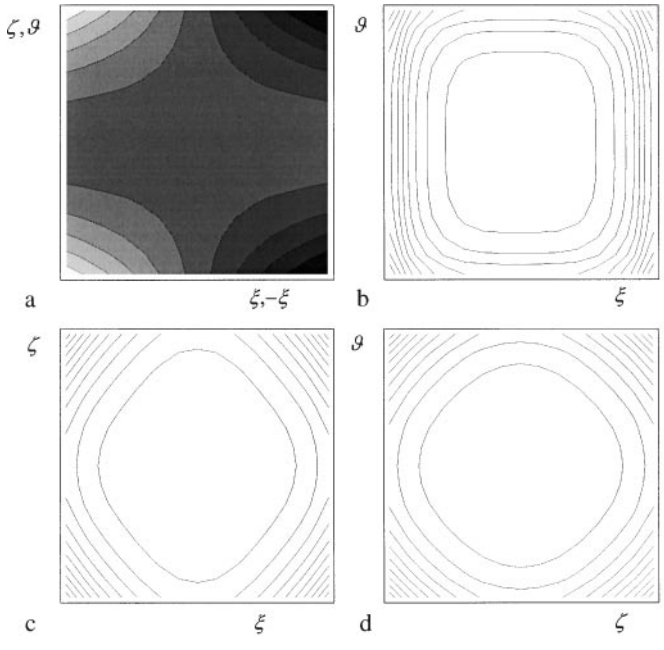

Fig. 8a–d. Curve families obtained by sectioning the surfaces defined **a** by Eq. (23) and **b–d** by Eq. (24) (see text for details)

that significant reconstructions can be obtained. Figures 9b–d show the second, third and fourth local moments, calculated with $T^+ = 10$ and 100 for the tract of the series $Re = 7000$ already previously considered. The local fourth-order moment, despite having a similar behaviour to that of the local variance, proves to be a bit more selective in identifying large scale intermittences, as one can see from the low level of base noise in the tracts with small scale fluctuations. Even more interesting is the local third-order moment that, by keeping the sign of the deviation, allows us to distinguish the sign of fluctuation with respect to the local mean values. In the presence of a brusque variation of velocity, it performs a double oscillation: if the gradient is positive, it first has positive peak followed by a negative one, while the sequence is inverted if the gradient is negative. This is evident, for example, in the tract between $t^+ = 6200$ and 6450, where the local third-order moment, calculated with $T^+ = 100$ (note how by passing from $T^+ = 10$ to 100 the behaviour becomes more significant, loosing sensitivity to the brusque small scale fluctuations but at the same time highlighting those of the middle or large scales), prevents a marked double oscillation that in the time series corresponds to a double sequence of progressive decreasing in velocity followed by a sudden increase. Such behaviour brings to mind the multiple ejections burst (Tardu 1995) where sequences of one or more ejections of middle intensity are followed by a final very intense one, and suggests the employment of the local third-order moment, possibly associated to that of the second or fourth-order, to highlight the presence of sequences of events and make their classification and regrouping easier. As an example of this, Figs. 10a and b respectively show the projection in delay co-ordinates of the local third-order moment for the trace of Fig. 9c ($T+ = 100$) and the behaviour of the local fourth-order moment versus that of the third. These make the distinguishing characteristics of the dynamics during these multiple ejections evident and recall as previously discussed with reference to VITA, the possibility of a connection between bursting events and heteroclinic excursions (e.g. Newell et al. 1988; Aubry et al. 1988).

The evidence that VITA detections and high-order moment related events correspond to excursions of the system leaving the basic turbulent dynamics is particularly important from a physical point of view, because it supports the hypothesis of coherent structure as moments of simplification of the dynamics with respect to the non-organised turbulence (see e.g. the discussion and references in Porporato and Ridolfi 1997 and Perona et al. 1998). According to this idea, during coherent structure formation the system is attracted towards a state of lower dimension (i.e. coherent) from which in turn it is suddenly repelled due to the saddle-type nature of this low-dimension state. The present results are in agreement with the experimental evidence of low-dimension elements during bursting events reported in Porporato and Ridolfi (1997) and with the low-dimension description of the bursting oscillation given by Perona et al. (1998).

4 Conclusions

In this work, we have looked into the link between state space reconstruction and conditional sampling techniques,

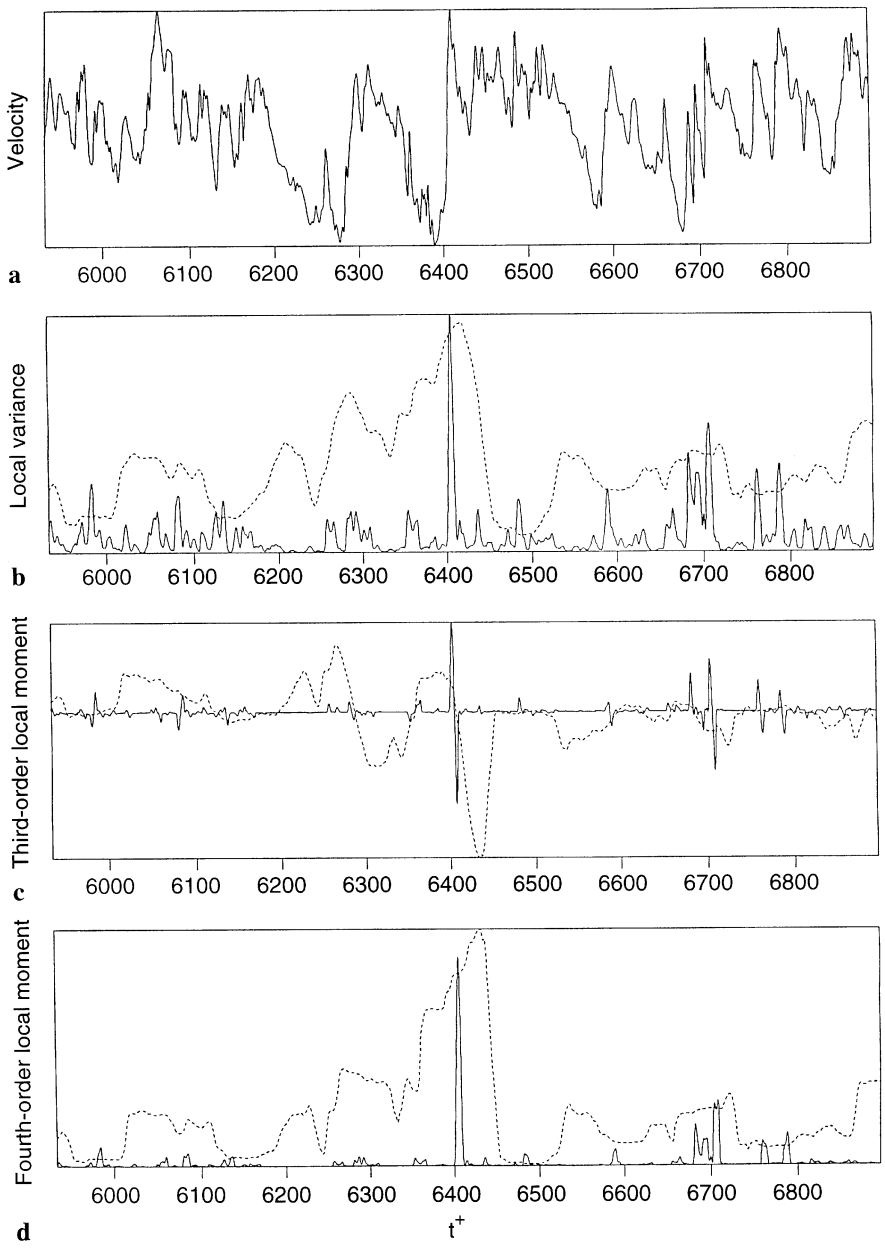

Fig. 9. **b**–**d** Traces of the local moments relative to the velocity trace shown in **a**. Solid lines refer to $T^+ = 10$, broken lines to $T^+ = 100$. **b** Local variance; **c** local third and **d** fourth-order moments

observing that the most effective conditional sampling techniques implicitly put a stage in which a kind of state space reconstruction is performed before the actual conditional sampling. The discussion has primarily concerned the VITA method, i.e. local variance, and the other main local statistical moments. The geometrical interpretation in the embedding space has given the possibility to better understand certain typical features of the method as well as offered an initiative towards a more objective choice of parameters directly based on the available series. Naturally, other methods of conditional sampling are amenable to similar interpretations, as well as various extensions considering different surfaces in the embedding space or different methods of reconstruction can be obtained.

From a physical point of view, observing that VITA events in the embedding space correspond to excursions of the system leaving the basic turbulence supports the idea of coherent structures as phases of dynamical simplification as hypothesised in the model by Newell et al. (1988) and in other low-dimensional models of the bursting cycle (see Perona et al. 1998 and references therein).

Methods from nonlinear time series analysis could have numerous applications in turbulence studies. The employment of the methods for state space reconstruction, for example, could be useful for multivariate turbulent series or for multi-point measurements in the identification and the study of spatiotemporal dynamics of coherent structures (Afraimovich et al. 1992; Healey 1993) or in the investigation of

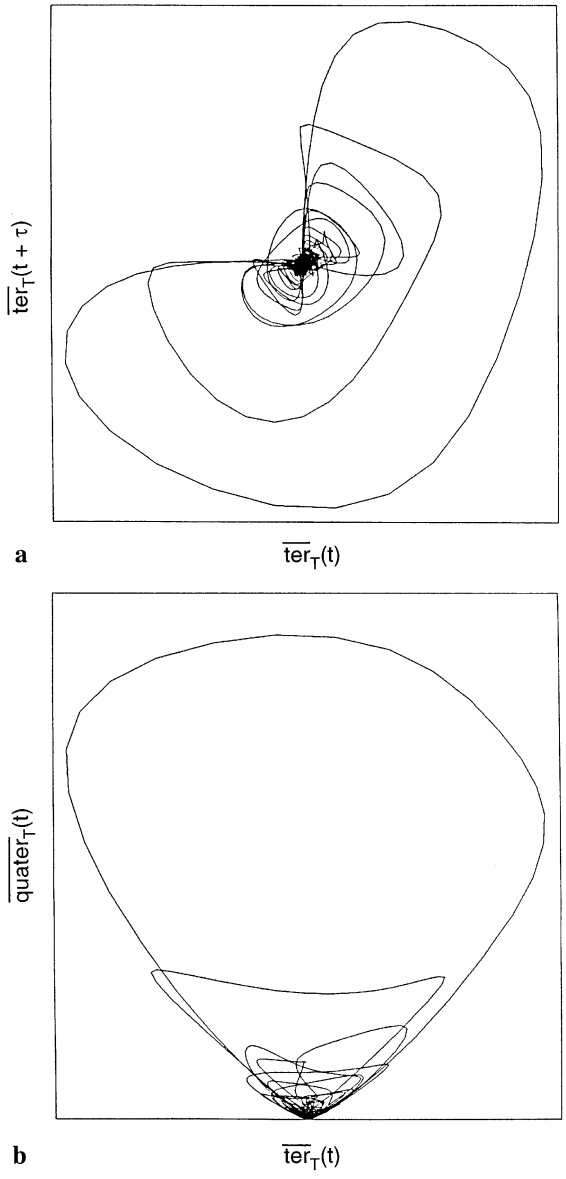

Fig. 10. **a** Two-dimensional reconstruction of the local third-order moment trace shown in Fig. 9c with the broken line. **b** Local fourth-order moment versus the third (broken lines of Fig. 9d and 9c respectively)

nonlinear correlations in flow fields (Prichard and Theiler 1995).

References

Abarbanel HDJ; Brown R; Sidorovich JJ; Tsimring LS (1993) The analysis of observed chaotic data in physical systems. Rev Mod Phys 65: 1331–1392

Afraimovich VS; Ezersky AB; Rabinovich MI; Shereshevsky MA; Zheleznyak AL (1992) Dynamical description of spatial disorder. Physica D 58: 331–338

Alfredsson PH; Johansson AV (1984) On the detection of turbulence-generating events. J Fluid Mech 139: 325–345

Antonia RA (1981) Conditional sampling in turbulence measurement. Ann Rev Fluid Mech 13: 131–156

Aubry N; Holmes P; Lumley JL; Stone E (1988) The dynamics of coherent structures in the wall region of a turbulent boundary layer. J Fluid Mech 192: 115–176

Blackwelder RF; Kaplan RE (1976) On the wall structure of the turbulent boundary layer. J Fluid Mech 76: 89–112

Bonnet JP (Ed.) (1995) Eddy structure identification techniques for turbulent shear flows. CISM Course series 353. Springer Verlag, Wien

Buzug TH; Pfister P (1992) Comparison of algorithms calculating optimal embedding parameters for delay time coordinates. Physica D 58: 127–137

Casdagli M; Eubank S; Farmer JD; Gibson J (1991) State space reconstruction in the presence of noise. Physica D 51: 52–98

Cross MC; Hohenberg PC (1993) Pattern formation outside of equilibrium. Rev Mod Phys 65: 851–1112

Gibson JF; Farmer JD; Casdagli M; Eubank S (1992) An analytic approach to practical state space reconstruction. Physica D 57: 1–30

Grassberger P; Schreiber TH; Schaffrath C (1991) Nonlinear time sequence analysis. Int J Bifurcation and Chaos 1: 521–547

Healey JJ (1993) A dynamical systems approach to the early stages of boundary-layer transition. J Fluid Mech 255: 667–681

Hussain F (1986) Coherent structures and turbulence. J Fluid Mech 173: 303–356

Jeong J; Hussain F; Schoppa W; Kim J (1997) Coherent structures near the wall in a turbulent channel flow. J Fluid Mech 332: 185–214

Johansson AV; Alfredsson PH (1982) On the structure of turbulent channel flow. J Fluid Mech 122: 295–314

Keefe LR (1988) Connecting coherent structures and strange attractors. In: New-Wall Turbulence (Eds. SJ Kline, NH Afgan) 63–80 Hemisphere Publishing Corporation, New York

Landahl MT (1990) On sublayer streaks. J Fluid Mech 212: 593–614

Lu SS; Willmarth WW (1973) Measurement of the structure of the Reynolds stress in a turbulent boundary layer. J Fluid Mech 60: 481–511

Luchik TS; Tiederman WG (1987) Timescale and structure of ejections and bursts in turbulent channel flows. J Fluid Mech 174: 529–552

Newell C; Rand A; Russel D (1988) Turbulent transport and the random occurrence of coherent events. Physica D 33: 281–303

Packard NH; Cructchfield JP; Farmer JD; Shaw RS (1980) Geometry from a time series. Phys Rev Lett 45: 712–716

Perona P; Porporato A; Ridolfi L (1998) A simple experimental equation for the bursting cycle. Phys Fluids 10: 3023–3026

Porporato A; Ridolfi L (1997) Nonlinear analysis of near-wall turbulence time series. Appl Sci Res 57: 235–261

Prichard D; Theiler J (1995) Generalized redundancies for time series analysis. Physica D 84: 476–493

Robinson SK (1991) Coherent motions in the turbulent boundary layer. Ann Rev Fluid Mech 23: 601–624

Rosenstein MT; Collins JJ; De Luca CJ (1994) Reconstruction expansion as a geometry-based framework for choosing proper delay times. Physica D 73: 82–98

Sauer T; Yorke JA; Casdagli M (1991) Embedology. J Stat Phys 65: 579–616

Takens F (1981) Detecting strange attractors in turbulence. In: Lectures Notes in Mathematics, Vol. 898, Berlin, Springer

Tardu S (1995) Characteristics of single and clusters of bursting events in the inner layer; Part 1: Vita events. Exp Fluids 20: 112–124

Tennekes H; Lumley JL (1972) A first course in turbulence (The MIT Press, Cambridge)

Yuan YM; Mokhtarzadeh-Dehghan MR (1994) A comparison study of conditional-sampling methods used to detect coherent structures in turbulent boundary layers. Phys Fluids 6: 2038–2057